

# Hydrothermal synthesis and characterization of hexagonal and monoclinic neodymium orthophosphate single-crystal nanowires

Hangmin Guan<sup>a</sup> and Youjin Zhang<sup>b,\*</sup>

<sup>a</sup>Department of Chemistry, University of Science and Technology of China, Hefei 230026, PR China

<sup>b</sup>Department of Food Science and Engineering, University of Science and Technology of China, 121 MeiLin Road, Hefei 230052, PR China

Received 14 July 2003; received in revised form 25 August 2003; accepted 7 September 2003

## Abstract

Hexagonal and monoclinic  $\text{NdPO}_4$  nanowires about 5–50 nm in diameter and up to several micrometers long were prepared through hydrothermal reaction in 100°C and 220°C, respectively. The products were characterized by X-ray diffraction (XRD), transmission electron microscopy (TEM), X-ray photoelectron spectra (XPS), and high-resolution transmission electron microscopy (HRTEM). Furthermore, both the temperature and the pH value influence on the products were investigated.

© 2003 Elsevier Inc. All rights reserved.

**Keywords:** Crystal morphology; Low dimensional structures; Hydrothermal crystal growth; Phosphates

## 1. Introduction

Nanowires and nanobelts representing a class of quasi-one-dimensional (1D) nanostructures are the focus of much attention because of their novel physical properties that are quite different from those of their corresponding bulk materials [1,2]. These new nanoscale materials have potential applications in mesoscopic research and development of nanodevices [3,4]. Many kinds of nanowires (nanobelts) have been fabricated by different methods [5–7].

Recently, much attention has been paid to the preparation of rare-earth orthophosphate nanomaterials [8–10]. Structural and chemical stability, long-term corrosion resistance, and high melting point of rare-earth orthophosphate make these materials suitable for use as heat-resistant and ceramic materials and as a primary encapsulation medium for the permanent disposal of certain types of radioactive wastes, such as  $\text{U}^{4+}$  and  $\text{Th}^{4+}$  [11–13]. Rare-earth activated luminescence in lanthanide orthophosphates makes these materials potential candidates for application as a phosphor that is a highly efficient emitter of green light and lasers [14,15].

$\text{NdPO}_4$  is one of the rare-earth orthophosphate, which has application in laser physics, and can be heat-resistant and ceramic materials [16,17]. In addition, hexagonal  $\text{NdPO}_4$  can be applied in the tribology because of its natural layered structure [18]. However, to best of our knowledge, no studies have focused on the synthesis of  $\text{NdPO}_4$  nanowires either monoclinic or hexagonal. Only Kaya and co-workers reported the product of monoclinic  $\text{NdPO}_4$  nanoparticles by the direct chemical reaction [17].  $\text{NdPO}_4$  would be of great significance because of the possible novel properties induced by their reduced dimensionality. Herein we report the synthesis of hexagonal and monoclinic neodymium orthophosphate nanowires by a hydrothermal synthetic pathway.

## 2. Experiment

In the typical preparation of hexagonal  $\text{NdPO}_4$  nanowires, 0.168 g  $\text{Nd}_2\text{O}_3$  was first dissolved in 5 mL 1 M  $\text{HNO}_3$ , and then 5 mL 0.1 M  $\text{Na}_3\text{PO}_4$  solution was added. The pH value of the solution was adjusted to 1.0 under stirring by 0.1 M  $\text{NaOH}$ . The above solution was transferred into a stainless steel autoclave with inner Teflon vessel (volume, 50 mL) and distilled water was added until about 80% of the autoclave capacity was

\*Corresponding author. Fax: +86-551-3492140.

E-mail address: [zyj@ustc.edu.cn](mailto:zyj@ustc.edu.cn) (Y. Zhang).

filled. After the autoclave was sealed, it was maintained at 100°C for 3 h and then was naturally cooled to room temperature. After the sample was washed three times with distilled water and absolute alcohol and vacuum-dried at 60°C for 6 h, the white precipitates were obtained. Similarly, monoclinic NdPO<sub>4</sub> was prepared at 220°C for 3 h.

The two samples were characterized by X-ray diffraction (XRD), employing a scanning rate of 0.05° s<sup>-1</sup> with 2θ from 10° to 70° and using an MXP18AHF X-ray diffractometer (MAC Science Co. Ltd.) equipped with graphite monochromatized CuKα radiation (λ = 0.15418 nm). The morphology and particle sizes of the sample were determined by Hitachi Model H-800 transmission electron microscopy (TEM) performed at 200 kV. The selected area electronic diffraction (SAED) and the crystallinity of individual nanowires were analyzed with a JEOL 2010 high-resolution transmission electron microscopy (HRTEM) running at 200 kV. In order to identify the valence states of neodymium and phosphorus, the X-ray photoelectron spectra (XPS) were used, which were performed on an ESCALAB MK II X-ray photoelectron spectrometer, using a MgKα radiation as the exciting source.

### 3. Results and discussion

Phase identification of the as-prepared samples was carried out using the XRD pattern (Fig. 1). All diffraction peaks could be indexed to the hexagonal phase (Fig. 1a) and the monoclinic phase (Fig. 1c). No obvious impurity phase was found. The shape of the diffraction peaks suggested that the samples should be well crystallized. The calculated lattice parameters

of two phases extracted from the XRD data (hexagonal:  $a_1 = 0.6982$  nm,  $c_1 = 0.6351$  nm; monoclinic:  $a_2 = 0.6729$ ,  $b_2 = 0.6964$ ,  $c_2 = 0.6384$  nm and  $\beta = 103.58^\circ$ ) were consistent with the literature data in the JCPDS file (hexagonal,  $a_1 = 0.6981$  nm,  $c_1 = 0.6342$  nm; monoclinic,  $a_2 = 0.6735$ ,  $b_2 = 0.6959$ ,  $c_2 = 0.6405$  nm and  $\beta = 103.68^\circ$ ).<sup>1</sup>

The temperature dependence of the reaction was investigated. When the reaction temperature was 100°C, only the hexagonal phase could be found (Fig. 1a). At about 200°C, the new phase appeared although hexagonal phase seemed to remain the main phase. This new phase could be indexed as the monoclinic NdPO<sub>4</sub> (Fig. 1b). When the reaction temperature arrived at 220°C, the XRD indicated that the hexagonal sample had completely transformed into the monoclinic phase (Fig. 1c). When temperature was above 220°C, the better crystallinity but larger crystallite size of the whiskers were generated.

The typical TEM and HRTEM images of the samples are illustrated in Fig. 2. Hexagonal (Fig. 2a) and monoclinic (Fig. 2b) NdPO<sub>4</sub> crystals both displayed nanowire morphology with diameters from 5 to 50 nm and lengths exceeding several micrometers. As shown in the inset Fig. 2c and d, the selected area electronic diffraction (SAED) patterns of the sample were consistent with the high crystallinity, and the diffraction spots could be indexed as the hexagonal phase and the monoclinic phase, respectively. Those results were in good agreement with the results of XRD. The HRTEM images are shown in Fig. 2e and f. The fringe spacing about 0.630 nm observed in the Fig. 2e agrees with the separation between the (0001) lattice planes of the hexagonal phase and nanowires grown in a [0001] direction. In Fig. 2f, the growing direction of the monoclinic NdPO<sub>4</sub> nanowires is perpendicular to the [110] direction and the fringe spacing in Fig. 2f was about 0.467 nm, which corresponded to the [110] plane of monoclinic NdPO<sub>4</sub> (see footnote 1).

The influence of pH value on the morphology of NdPO<sub>4</sub> was investigated. It had been found that the morphologies of product intensively dependent on the pH value in the solution. When the pH < 1, hexagonal and monoclinic NdPO<sub>4</sub> morphology was nanowire. However when the pH > 1, no nanowires were obtained in the products and only nanorods could be found in the final product.

In all experiments, the pH value of the solution was adjusted by 0.1 M NaOH solution under stirring before the hydrothermal reaction, during which when the pH > 1, the white precipitation appeared in the originally clear and colorless solution and the quantity of the white precipitation dramatically increased with

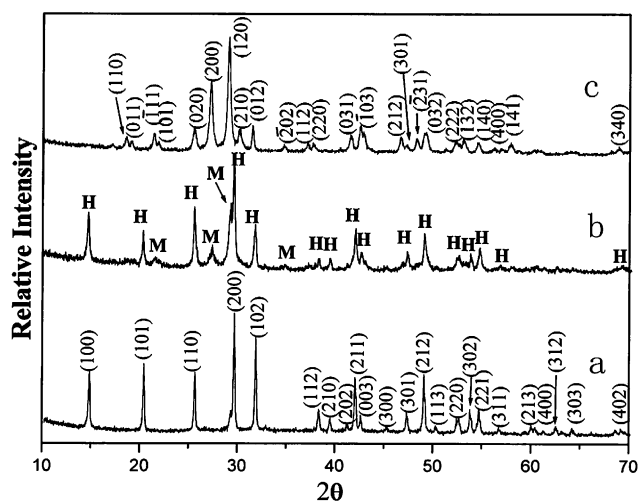


Fig. 1. XRD patterns of NdPO<sub>4</sub> nanowires: (a) 100°C-hexagonal, (b) 200°C (H: hexagonal phase; M: monoclinic phase), (c) 220°C-monoclinic.

<sup>1</sup>JCPDS Files No. 75-18882 for hexagonal NdPO<sub>4</sub>; JCPDS Files No. 83-654 for monoclinic NdPO<sub>4</sub>.

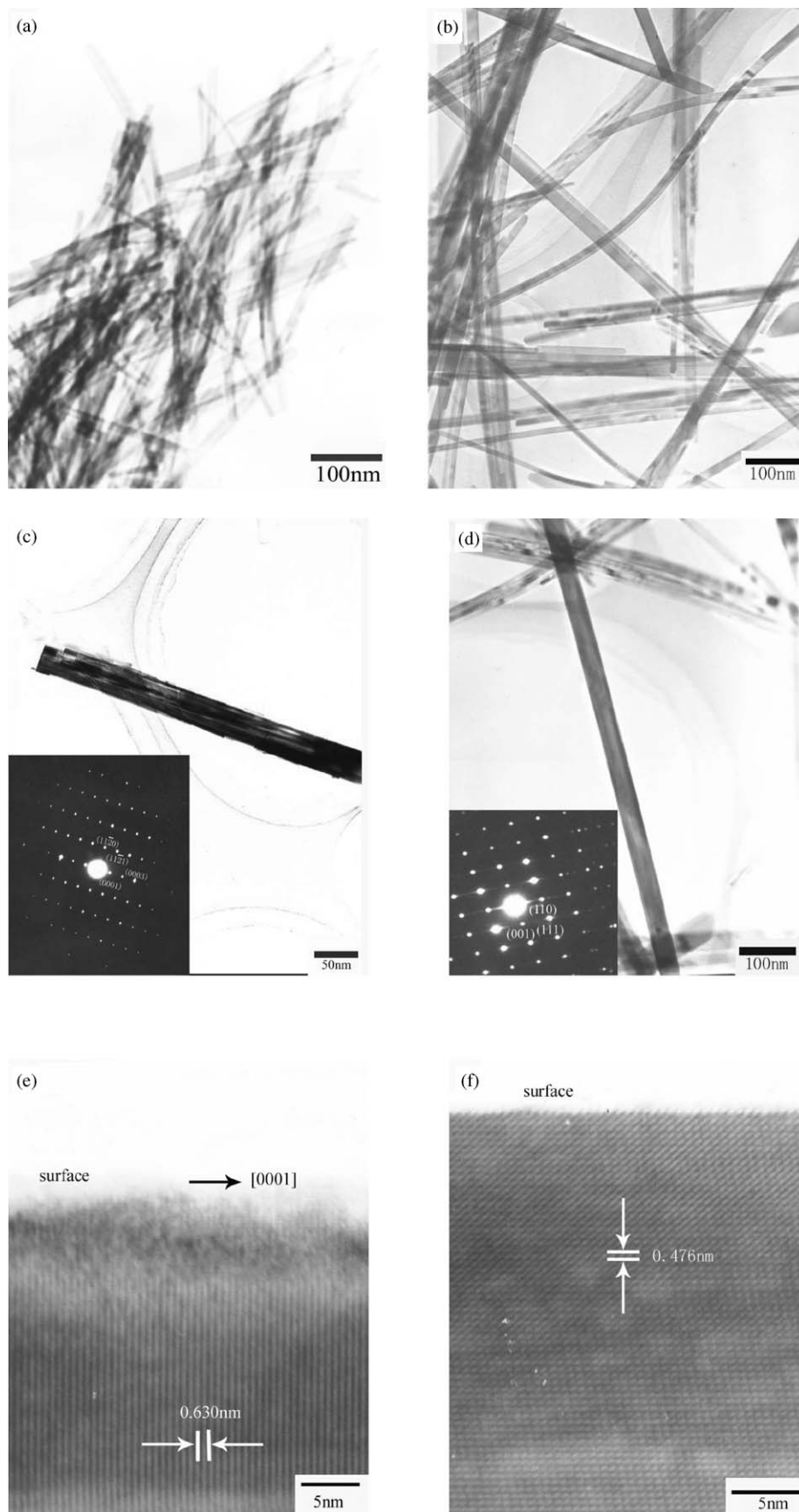
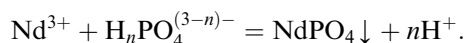


Fig. 2. TEM and HRTEM images of hexagonal and monoclinic  $\text{NdPO}_4$ : (a) TEM image of hexagonal  $\text{NdPO}_4$  nanowires, (b) TEM image of monoclinic  $\text{NdPO}_4$  nanowires, (c) SAED pattern along  $[1\bar{1}0]$  zone axis of hexagonal  $\text{NdPO}_4$  nanowires and corresponding image, (d) SAED pattern along  $[1\bar{1}0]$  zone axis of monoclinic  $\text{NdPO}_4$  nanowires and corresponding image, (e) HRTEM image of hexagonal  $\text{NdPO}_4$  nanowires, (f) HRTEM image of monoclinic  $\text{NdPO}_4$  nanowires.

increasing pH. However, if the pH of the above solution was continually adjusted by lowering with 0.1 M HCl solution, the quantity of the white precipitation dramatically decreased. Finally, when  $\text{pH} \leq 1$ , the solution became the clear and colorless solution again. Obviously, the white precipitation could be dissolved in the acid solution. The white precipitation was proved as an amorphous substance including  $\text{PO}_4^{3-}$  and  $\text{H}_2\text{O}$  by XRD and IR spectra.

So in the hydrothermal synthesis, the main reaction may take place as follows:



In experiments,  $\text{NdPO}_4$  prepared at  $100^\circ\text{C}$  possessed a hexagonal crystal structure. It is well known that the hexagonal crystal structure, such as ZnO and CdSe, often shows the anisotropic growth along the [001] direction [19,20]. So it is the anisotropic growth that is believed to be the inherent driving force in the growing process of the hexagonal nanowires [21]. Peng et al. have demonstrated that a higher chemical potential is favorable for 1D nanomaterials growth [21, 22]. Meanwhile, faster ionic motion usually ensures a reversible pathway between the fluid phase and solid phase and allows ions to adopt correct positions in developing crystal lattices [23]. Thus, when the pH value of the solution is alkaline, there are a great deal of the white precipitation in the solution, which led to low  $\text{Nd}^{3+}$  and  $\text{H}_n\text{PO}_4^{(3-n)-}$  concentration, low chemical potential and slow ion motion. These are not favorable for the product of the 1D nanomaterials. On the contrary, as the pH value of the solution was lowered and the white precipitation was gradually dissolved resulting in high

$\text{Nd}^{3+}$  and  $\text{H}_n\text{PO}_4^{(3-n)-}$  concentration, which implies high chemical potential and the fast ion motion in the solution. Finally, when the  $\text{pH} < 1$ , the precipitation was completely dissolved to form the clear and colorless solution in which the chemical potential and the speed of the ion motion both arrived at the maximum value. Considering the above factors, hexagonal  $\text{NdPO}_4$  nanowires can be grown in the acid environment especially  $\text{pH} < 1$ .

Monoclinic  $\text{NdPO}_4$  nanowires might derive from hexagonal  $\text{NdPO}_4$  nanowires. That is, with the reaction temperature rising, hexagonal  $\text{NdPO}_4$  nanowires were firstly produced, and then hexagonal phase nanowires might transform into monoclinic phase at about  $200^\circ\text{C}$ . This process can be understood as in situ phase change in a nanowire similar to the phase transitions in the  $\text{Cu}_2\text{S}$  nanowires [24]. Some kind of subtle or dramatic topological effect that was caused by a phase transition within a nanowire may result in some coiling of the monoclinic nanowires (as shown in Fig. 2b).

The XPS spectra are shown in Figs. 3 and 4. As shown in Fig. 3a (hexagonal) and Fig. 4a (monoclinic), there were no obvious impurities on the surface of the samples. Referring to the data collected in literatures [25,26], the two spectra indicate that the phosphorus exists completely in the form of  $\text{PO}_4^{3-}$  and neodymium exists as Nd(III) in all samples. As shown in the inset Fig. 3b and c, the binding energy for the P  $2p_{3/2}$  of  $\text{PO}_4^{3-}$  is 132.70 eV and for the Nd  $3d_{5/2}$  orbital of Nd(III) it is 982.80 eV in the hexagonal phase. In the Fig. 4b and c, the binding energy for the P  $2p_{3/2}$  of  $\text{PO}_4^{3-}$  is 133.25 eV and for the Nd  $3d_{5/2}$  orbital of Nd(III) it is 982.75 eV.

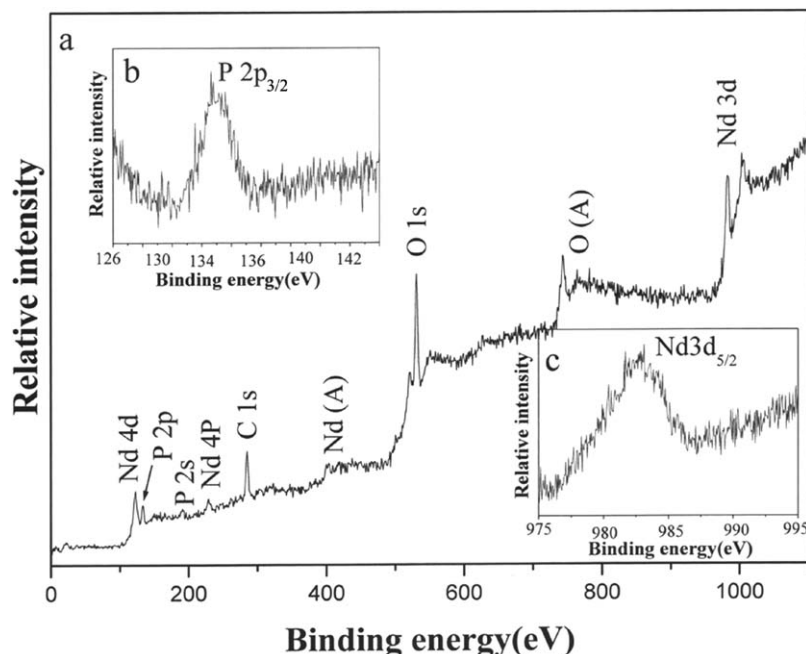


Fig. 3. X-ray photoelectron spectra (XPS) analysis of hexagonal  $\text{NdPO}_4$  nanowires: (a) Survey spectrum, (b) P  $2p_{3/2}$  region, (c) Nd  $3d_{5/2}$  region.

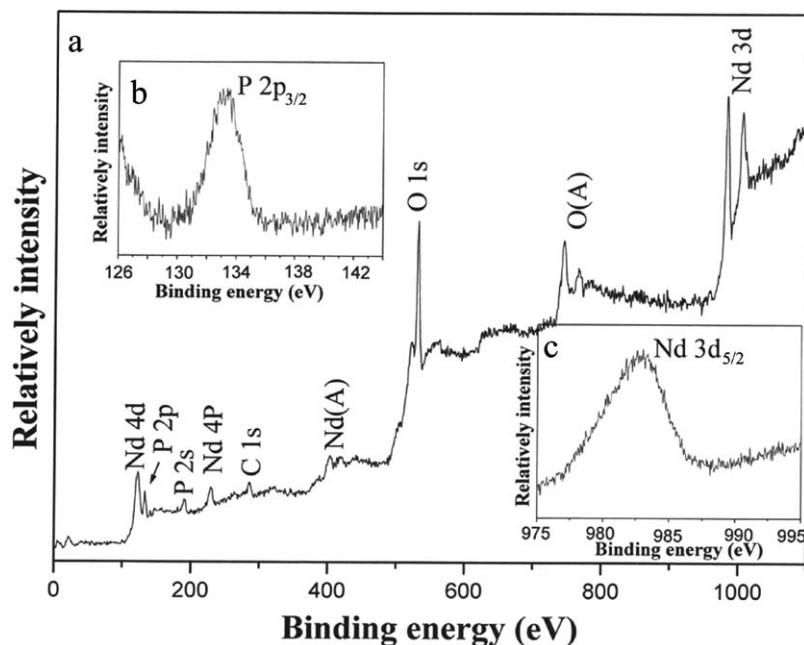


Fig. 4. X-ray photoelectron spectra (XPS) analysis of monoclinic NdPO<sub>4</sub> nanowires: (a) Survey spectrum, (b) P 2p<sub>3/2</sub> region, (c) Nd 3d<sub>5/2</sub> region.

#### 4. Conclusion

In summary, two structures of NdPO<sub>4</sub> nanowires were successfully synthesized by a hydrothermal method at 100°C and 220°C. The temperature and the pH value influence on the product were investigated. The possible growth process of NdPO<sub>4</sub> nanowires was also discussed. XRD, HRTEM, TEM and XPS investigations on these nanowires had been carried out. Our experiment results demonstrate that this common hydrothermal method can successfully produce high-quality crystalline nanowires.

#### References

- [1] X. Fduan, Y. Huang, Y. Cui, J.F. wang, C.M. Lieber, *Nature* 409 (2001) 66.
- [2] A.P. Alivisatos, *Science* 271 (1996) 933.
- [3] G. Fasol, *Science* 280 (1998) 545.
- [4] M.H. Huang, S. Mao, H. Feick, H.Q. Yan, Y.Y. Wu, H. Kind, E. Weber, R. Russo, P.D. Yang, *Science* 292 (2001) 1897.
- [5] T.J. Trentlet, K.M. Hickman, S.C. Goel, A.M. Viano, P.C. Gibbons, W.E. Buhro, *Science* 270 (1995) 1791.
- [6] X. Duan, M.C. Lieber, *Adv. Mater.* 12 (2000) 298.
- [7] Y. Li, G.W. Meng, L.D. Zhang, F. Phillipp, *Appl. Phys. Lett.* 76 (2000) 2011.
- [8] K. Meyssamy, R. Karsten, K. Andreas, N. Sabine, H. Markus, *Adv. Mater.* 11 (1999) 840.
- [9] K. Riwozki, H. Meyssamy, A. Koronwski, M. Haase, *J. Phys. Chem. B* 104 (2000) 2824.
- [10] Y.J. Zhang, H.M. Guan, *J. Cryst. Growth* 256 (2003) 156.
- [11] M.M. Abraham, L.A. Boatner, T.C. Quinby, D.K. Thomas, M. Rappaz, *Radioactive Waste Manmge.* 1 (1980) 181.
- [12] L.A. Boatner, G.W. Beall, M.M. Abraham, C.B. Frinch, R.J. Floran, P.G. Hurray, M. Rappaz, in: *Management of Alpha-contaminated Wastes*, IAEA-SM-246/73, IALEA, Vienna, 1981, p. 411.
- [13] Y. Hikichi, T. Nomura, *J. Am. Ceram. Soc.* 70C (1987) 252.
- [14] G. Blasse, A. Birl, *J. Chem. Phys.* 50 (1969) 2974.
- [15] J.R. Thronton, *Appl. Opt.* 8 (1969) 1087.
- [16] C. Zaldo, M. Rico, M.J. Martin, J. Massons, M. Aguilo, F. Diaz, *J. Lumin.* 79 (1998) 127.
- [17] C. Kaya, E.G. Bulter, A. Selcuk, A.R. Boccaccini, M.H. Lewis, *J. Eur. Ceram. Soc.* 22 (2002) 2333.
- [18] Y.F. Lian, H.X. Dang, *Tribology.* 13 (2) (1993) 183.
- [19] L. Vayssieres, *Adv. Mater.* 15 (5) (2003) 464.
- [20] Z.A. Peng, X.G. Peng, *J. Am. Chem. Soc.* 123 (2001) 1389.
- [21] X. Wang, Y.D. Li, *Angew. Chem. Int. Ed.* 41 (24) (2002) 4790.
- [22] Z.A. Peng, X.G. Peng, *J. Am. Chem. Soc.* 124 (2002) 3343.
- [23] T.J. Trentler, K.M. Hickman, S.C. Goel, A.M. Viano, P.C. Gibbons, W.E. Buhro, *Science* 270 (1995) 1791.
- [24] S.H. Wang, L. Guo, X.G. Wen, S.H. Yang, J. Zhao, J. Liu, Z.H. Wu, *Mater. Chem. Phys* 75 (2002) 32.
- [25] C.D. Wagner, W.M. Riggs, L.E. Davis, J.F. Moulder, G.E. Muilenberg, *Handbook of X-ray Photoelectron Spectroscopy*, Perkin-Elmer Corporation, New York, CT, 1979.
- [26] Y. Uwamino, Y. Ishizuka, H. Yammatara, *J. Electron. Spectrosc. Relat. Phenom.* 34 (1984) 69.